IN-SITU DAMAGE DETECTION IN GLASS FIBRE COMPOSITES

S. A. Malik, S. O. Ojo, D. Harris and G. F. Fernando*
School of Metallurgy and Materials, University of Birmingham,
Edgbaston, Birmingham, B15 2TT. United Kingdom.
*g.fernando@bham.ac.uk

SUMMARY

This paper reports on further development of the technique to use reinforcing glass fibres as light-guides to enable *in-situ* detection of fibre fracture. A high-speed camera was used to record the fracture of individual reinforcing fibres during mechanical loading.

Keywords: Damage detection, Fibre fracture, Image analysis, Self-sensing

INTRODUCTION

The authors have demonstrated previously that conventional reinforcing glass fibres can be used as light-guides to facilitate chemical process monitoring [1, 2]. The authors have also used the light transmission characteristics through the reinforcing fibres to detect fracture of the fibres [3].

There are a number of advantages associated with the deployment of reinforcing fibres as sensors. For example: (i) a significant proportion of the optical fibre sensors reported in the literature have dimensions that are at least an order of magnitude larger than the reinforcing fibres. This diameter mismatch can induce significant distortions in the orientation of the reinforcing fibres [4]. This can lead to adverse effects on the compressive and fatigue properties of the composite; (ii) the reinforcing fibres can be used to obtain evanescent wave spectra. Therefore, the nature of specified functional groups or chemical reactions that take place on the surface of the glass fibre can be monitored. Moreover, the effects of chemical ageing or reactivity of coupling agents, such as silane, towards specified functional groups in the matrix can be studied in real-time; and (iii) the light transmission characteristics through the glass fibres can be used to infer the mechanical integrity of the reinforcement. Hence, it is possible to cross-correlate specified surface-treatment regimes to the cross-linking kinetics during processing and, subsequent fracture behaviour of the fibres during mechanical loading. In effect, the reinforcing glass fibres can provide information on the chemical and structural integrity of the composite throughout its lifetime.

In this present work, the tensile fracture behaviour of E-glass fibre bundles and their composites were investigated. Surface-mounted piezo-electric transducers were used to monitor the acoustic emissions generated during tensile loading. The first acoustic emission signal detected was used to trigger a high-speed camera to facilitate the acquisition of images of the polished end of the fibre bundle.

EXPERIMENTAL

Materials

The E-glass fibres used in this study were water-sized and supplied by PPG Industries (UK) Ltd. There were approximately 2500 filaments in each fibre bundle, with an average fibre diameter of 15 (± 3 μm). The refractive index of the E-glass pre-form was measured to be 1.56 at 589.6 nm and 20 °C. Custom-made optical fibres with an average diameter of 12 μm (± 1 μm) were used to develop and optimise the technique for *in-situ* damage detection using the reinforcing fibres.

A two-component resin system, EPO-TEK® 314, supplied by Promatech Ltd., was used as the matrix. The refractive index of the cured resin was 1.4965 (measured at 589 nm and 23 ºC). The resin and hardener were weighed in the required stoichiometric ratio of 100:6 (epoxy:amine) and mixed thoroughly prior to impregnating the E-glass fibre bundle. The impregnated fibre bundle was processed at 120 °C for 3 hours in an air-circulating oven.

Sample preparation

Two types of fibres were used for producing test specimens for tensile testing: as-received (un-impregnated) E-glass, and small-diameter optical fibres. Composite specimens were prepared from water-sized E-glass fibre bundles and the EPO-TEK® 314 resin. A schematic illustration of the technique that was used for fabricating void-free composite specimens is illustrated in Figure 1a. The method used involved the construction of a mould whereby the reinforcing fibres were sandwiched between two glass plates. The lengths of the top and bottom plates were 300 mm and 150 mm respectively; both plates were 30 mm wide and 6 mm thick. A release agent, Frekote® 700-NC (Loctite®, UK) was applied to the glass plates before assembly to allow easy removal of the composite after processing. Two rectangular moulds were formed between the glass plates using adhesive-backed PTFE release-film (Aerovac, UK) and secured to each plate. These moulds served to contain the resin, and had cavity dimensions of 150 mm (length), 25 mm (width) and 0.5 mm (depth). The glass fibres were secured in position on the bottom plate before the top plate was aligned with the mould. A needle attachment from a syringe was positioned and secured within the mould using RTV 3140 silicone resin (Dow Corning, UK). The glass plates were clamped in place and sealed along three edges using the silicone resin. The entire assembly was positioned vertically and the EPO-TEK® 314 resin system was injected via the syringe into the mould. Once the mould cavity was completely filled with the resin, the syringe was withdrawn and the needle entry sealed with the silicone resin. The mould assembly with the resin impregnated fibres was placed in an air-circulating oven at 120 °C for 3 hours.

After cooling to room temperature, the composite was removed from the mould. Since the mould was larger than the width of the reinforcing fibre bundle, it was necessary to polish the excess resin along the length of the specimen. Finally, the ends of the fibre bundle were potted into SMA-905 optical fibre connectors (Thorlabs, UK). The SMA connectors had an inner bore of 1.4 mm diameter and the potted connectors were polished on an automatic polisher (APC-8000, Senko, UK) using conventional procedures. Custom-designed mild-steel end-tabs were used to protect the fibres and to

facilitate tensile loading on a mechanical testing machine. Scotch-Weld 9323 adhesive (3M, UK) was used to secure the samples within the end-tab assembly. A schematic illustration of the end-tab design is shown in Figure 1b. A photograph of an end-tabbed composite sample with a pair of SMA connectors is presented in Figure 1c.

The tensile test specimens involving the as-received E-glass reinforcing fibre bundles and small-diameter optical fibre bundles were end-tabbed and SMA connectors were attached using the procedures described previously. The fibre bundles were 270 mm in length and 10 mm in "width", and they had a gauge length of 100 mm. The average "thickness" of the bundle was approximately 1 mm. Due care and attention was given to ensure that the tension in the individual filaments was similar; this could not be guaranteed given the number of filaments in the bundles (2500 ± 200 and 2800 ± 200 for E-glass and small-diameter bundles respectively).

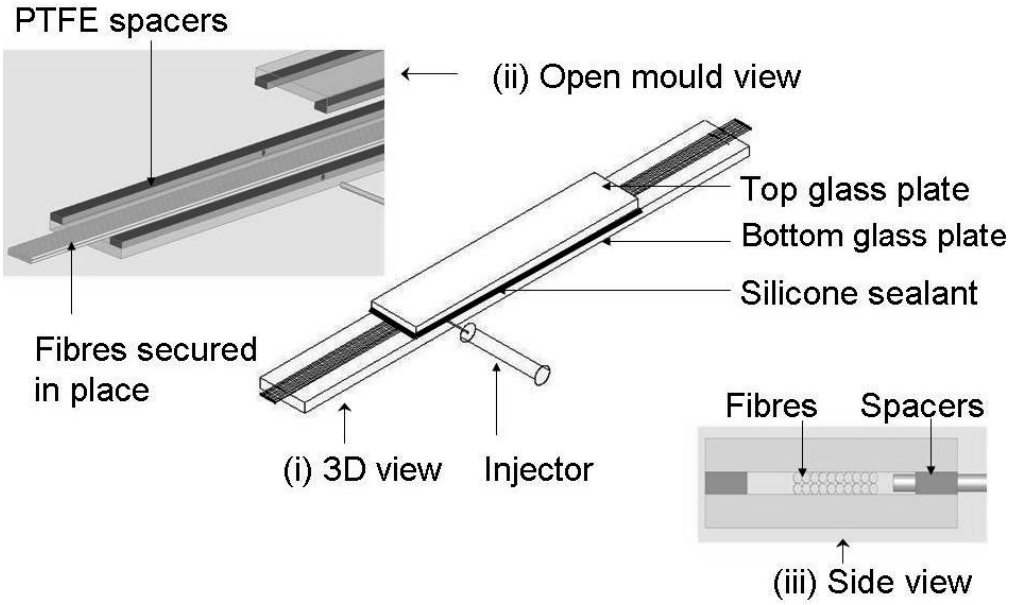

Figure 1a. Schematic illustration of the manufacturing process for the production of void-free composites: (i) 3-D view of the mould and sample; (ii) view of the open mould assembly showing the fibres and PTFE spacers; (iii) cross-sectional view of the mould assembly

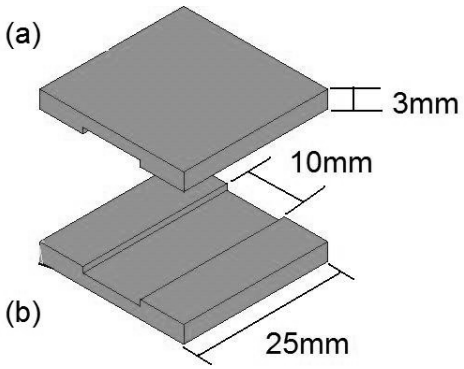

Figure 1b. A schematic illustration of the square end-tab assembly with cut-out sections to accommodate the fibres: (a) top and (b) bottom end-tabs.

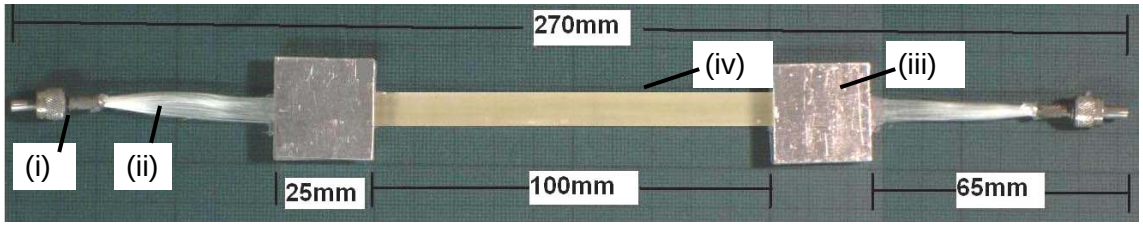

Figure 1c. Photograph of an E-glass composite sample with SMA connectors and end-tabs: (i) SMA connector; (ii) un-impregnated section of the E-glass fibre bundle; (iii) end-tab; (iv) void-free composite.

Tensile testing: The un-impregnated fibre bundles and the composites were loaded in tension on an Instron 5566 mechanical testing machine at a cross-head displacement rate of 1 mm per minute. A PC with a data acquisition system was used to record the applied load and the position of the cross-head. The tensile tests were carried out at room temperature.

Acoustic emission detection: A pair of Micro R15 piezo-electric transducers (Physical Acoustics Corporation, UK) was used to monitor acoustic emissions (AE) during tensile loading of the un-impregnated fibre bundles and composites. The AE transducers were attached to the fibre bundle and composite using a silicone gel (494-118, RS, UK). The AE data were recorded using propriety software. Prior to tensile testing of the composite specimens, AEs were simulated by fracturing a pencil lead to enable the calculation of the wave velocity and to ensure that the transducers were attached securely.

High-speed photography: A charge-coupled device (CCD) high-speed camera, FastCAM 1024 PCI (Photron, UK), was used to image one end of the fibre bundle, via the SMA connector, during tensile loading. A 200 mW green laser emitting at 532 nm was used to illuminate the opposite end of the E-glass fibre bundles and composites via an SMA connector. The small-diameter optical fibres were illuminated using a white light source (Intralux-4000, Warner Instruments, USA). The high-speed camera was operated at 60 frames per second. A lens attachment (12X Zoom Extender, Navitar, UK) was used with the high-camera to magnify the image. During the tensile loading of the test specimen, the high-speed camera was triggered by the first AE signal received by the piezo-electric transducer.

RESULTS AND DISCUSSION

Image analysis: The small-diameter optical fibres were used to develop the image analysis routines. The images obtained via the high-speed camera during tensile loading of the specimens were analysed using the image analysis routines in Matlab 8.0. A macro was developed that read the first image and identified each fibre as an individual entity; the centroidal position of each fibre was specified using x- and y-axis coordinates. For the remainder of the images obtained during tensile loading, the light intensity of each fibre was calculated using the same coordinate positions.

Figure 2a shows the first image that was captured at the start of the tensile test (t=0) involving the small-diameter optical fibres. Figure 2b represents the transposition of Figure 2a using the Matlab software. This step involved background-correction and adjustment of the luminance threshold using the software routines. Figure 2c is an x-y location plot after image processing in Matlab of the same image shown in Figures 2a and b. The quality and processing of the images presented in Figure 2c was found to be adequate to enable fracture of the reinforcing glass fibres to be studied. It was found that the Matlab routines are able to identify and process each individual fibre with an accuracy of 94 ±2 %.

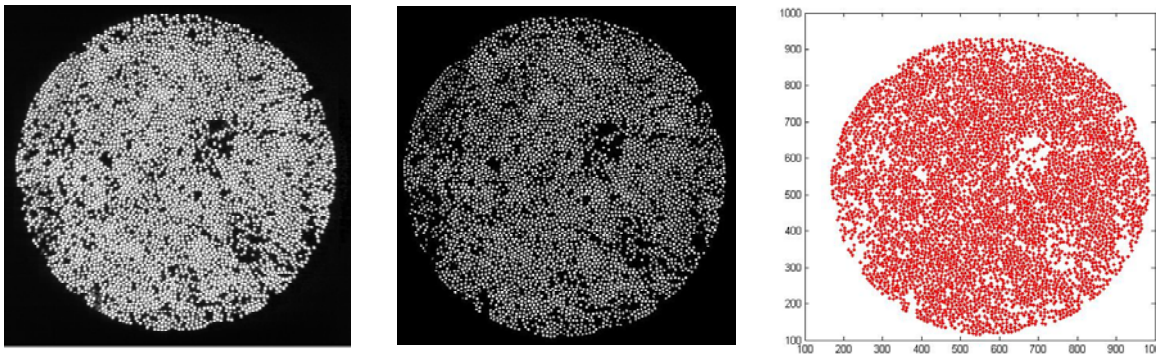

(a) First image (b) Background-corrected (c) X-y coordinates

Figures 2(a – c). Image analysis steps: (a) image from the high speed camera at t=0; (b) background-corrected image using Matlab routines; and (c) x-y plot for the location of individual fibres.

Figures 3 (a-d) show a series of images, generated using Matlab, corresponding to the 600th, 1800th, 3000th and 4800th frames captured by the high-speed camera during tensile testing of the small-diameter optical fibre bundle. The light intensity calculations for Figures 3 (a-d) are shown in Figures 3 (e-h) respectively where the x-and y-axes indicate the location of each fibre and the z-axis represents the light intensity at each location.

Tensile testing of fibre bundles: The image analysis routines developed can identify and track the survival or fracture of each fibre in the bundle during mechanical loading. The feasibility of using the image analysis routines to identify fibres, just prior to fracture, was investigated. Figures 4 (a-c) show three sequential frames during the tensile loading of the small-diameter optical fibre bundle; the arrow in each frame indicates the position of a fibre before, during and after fracture respectively. This trend was observed for all of the fibres, where an attenuation of the transmitted light intensity was observed just prior to failure.

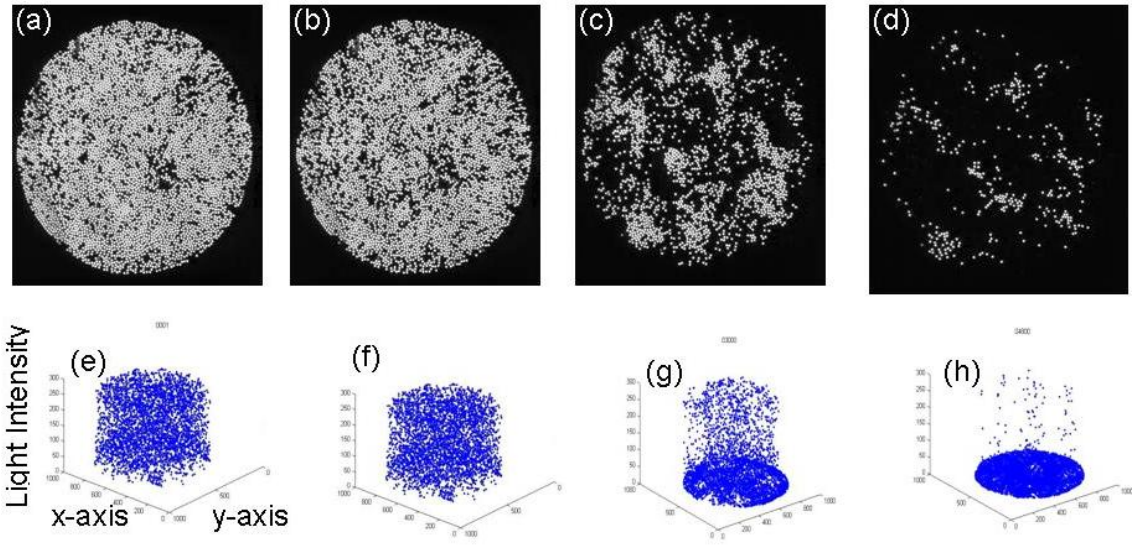

Figures 3 (a –h). Images captured by the high-speed camera (a-d) at different time intervals during tensile loading of the small-diameter fibre bundle: a) 10 seconds (frame 600); (b) 30 seconds (frame 1800); (c) 50 seconds (frame 3000); (d) 80 seconds (frame 4800); and the corresponding x-y location plots and light intensity (e-h), generated using Matlab.

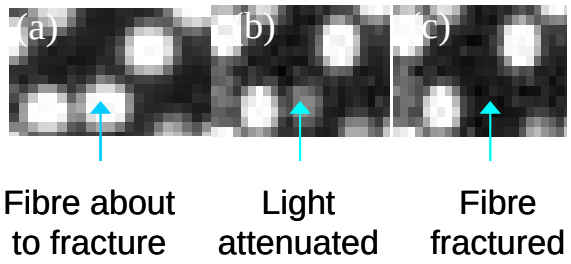

Figures 4 (a-c). Identification of an individual fibre by monitoring the transmitted light intensity: (a) whilst being loaded in tension; (b) just prior to fracture; (c) immediately after fibre fracture.

Figures 5 (a and b) show the relationships between the transmitted light intensity and applied load as a function of time for the small-diameter optical fibre bundle and as-received E-glass fibre bundle respectively. In the majority of cases, a rapid decrease in the transmitted light intensity was observed when 90 % or more of the applied load was reached. The failure of the un-impregnated fibre bundle was not catastrophic for the following reasons: (i) the tension of the fibres within the bundle was variable, (ii) the sequential nature of the failure of the weaker fibres means that upon failure the load is transferred to the surviving fibres; and (iii) the strength distribution of the fibres. The small, but noticeable, increase in the transmitted light intensity between approximately 60 and 80% of the applied load may be attributed to variations in the tension of the individual fibres in the bundle.

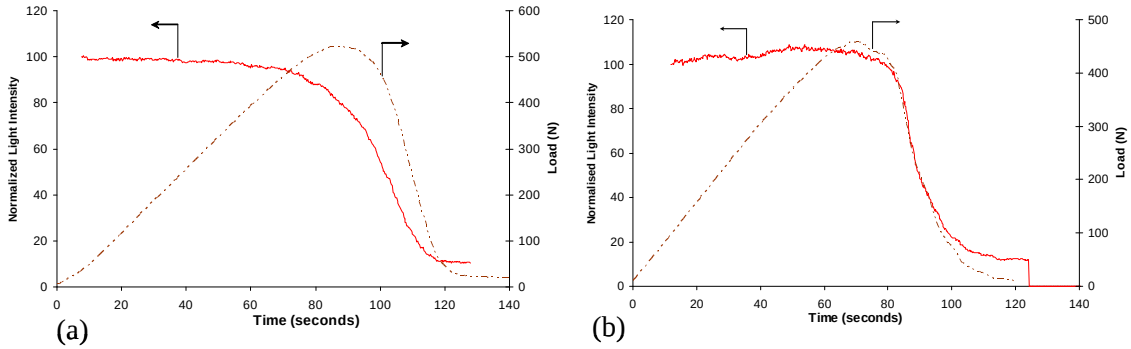

Figures 5 (a and b). Graphs showing the normalised transmitted light intensity and applied load as a function of time for: (a) a small-diameter optical fibre bundle; and (b) an E-glass fibre bundle.

Figures 6 (a and b) illustrate the load/time versus cumulative AE hits/time traces for the small-diameter optical fibre bundle and E-glass fibre bundle respectively. A characteristic feature for the fibre bundle is the continuation of acoustic emission after the peak-load has been reached. Since all the filaments in the bundle are not under the same tension, they are not loaded evenly. Furthermore, the filaments within the bundle have a distribution of tensile strengths.

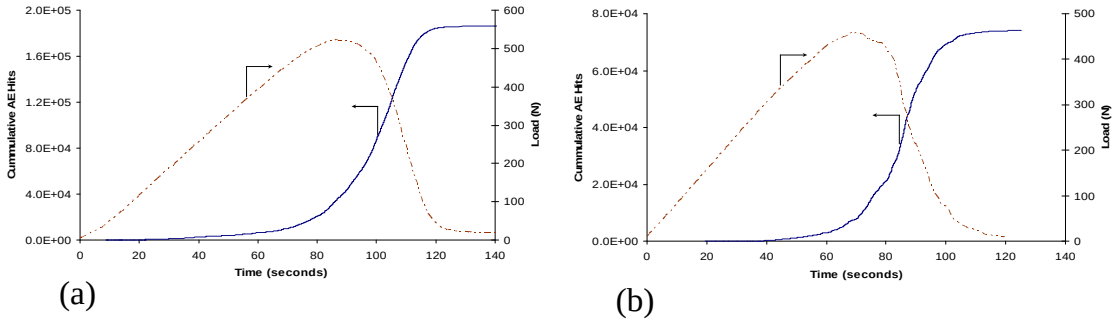

Figures 6 (a and b). Graphs showing the cumulative AE hits and load as a function of time for: (a) the small-diameter optical fibre bundle; and (b) the as-received E-glass fibre bundle.

Quality of composites: Figures 7(a-d) illustrate typical micrographs representing transverse sections of the composites manufactured from small-diameter optical fibres and E-glass reinforcing fibres. The fibre volume fractions, evaluated via image analysis, for the two composites were calculated to be 35-40% and 42-46% respectively. There was no evidence of voids in these composites. The fabrication procedure described previously was demonstrated to be a practical and viable technique for manufacturing void-free composites.

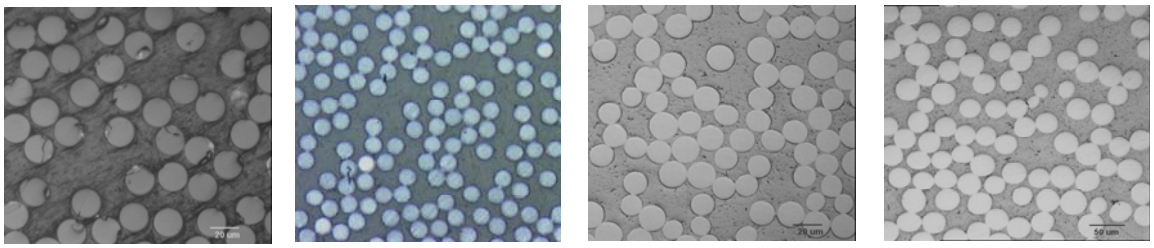

(a) (b) (c) (d)

Figures 7 (a-d): Typical micrographs representing transverse sections of composites manufactured using: (a-b) small-diameter optical fibres; and (c-d) E-glass fibres.

Tensile testing of composites: The fracture behaviour of the composites manufactured using the small-diameter optical fibres and E-glass fibres with the EPO-TEK® resin are shown in Figures 8 (a and b). The stress and cumulative AE hits as a function of time for the composites manufactured using as-received small-diameter optical fibres and E-glass fibres are shown in Figures 9 (a and b) respectively. The conclusion reached after testing twenty individual specimens was that the majority of the load/time traces were relatively linear up to failure. The cumulative AE hits for the as-received small-diameter optical fibre composite can be seen in Figure 9a, where a step-change in the AE activity is observed. This may be attributed to the fact that the fibres were used in the as-received state. Subsequent surface analysis revealed the presence of a high binder content on the surface of the fibres. The other contributing factors may be attributed to the development of longitudinal splitting and fibre fractures in the unidirectional composite. In contrast, a smoother exponential increase in the AE activity of the E-glass fibre composite was seen after approximately 40-50 % of the load. A less-noticeable step is observed for the as-received E-glass fibre composite when compared to the small-diameter fibre composite. In the case of the small-diameter optical fibre composites, the attenuation of the transmitted light was abrupt when the peak stress was reached. In the case of the E-glass fibre composite, a steady decrease was observed in the transmitted light intensity followed by an abrupt termination when the peak stress was reached.

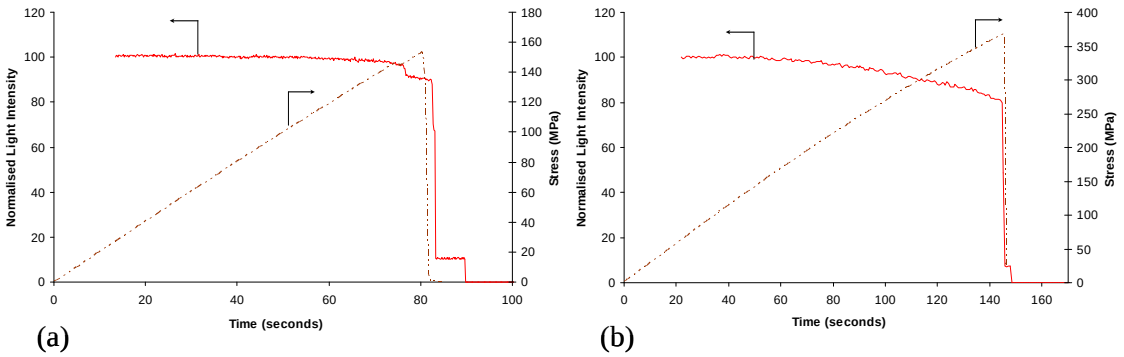

(a) (b)

Figures 8 (a and b). Graphs showing the normalised transmitted light intensity and applied load as a function of time for composites manufactured from: (a) small-diameter optical fibres; and (b) E-glass fibres.

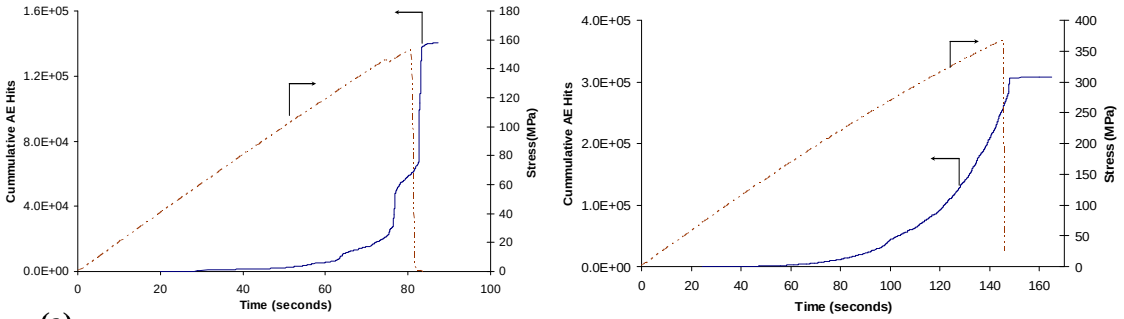

Figures 9 (a and b). Graphs showing the cumulative AE hits and applied stress as a function of time for composites manufactured from: (a) small-diameter optical fibres; and (b) E-glass fibres.

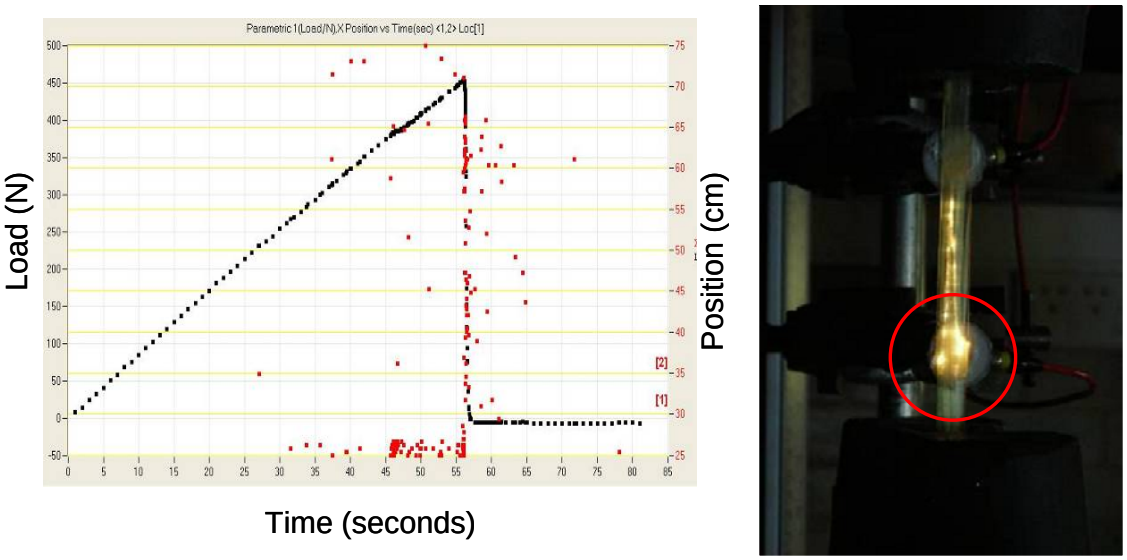

(a) AE location analysis and load trace with time

(b) Light bleeding through fractured self-sensing composite

Figures 10 (a and b). AE linear-location: (a) Graphs showing the location of AE hits as a function of load and time during tensile loading of a small-diameter optical fibre composite; and (b) image from a CCD camera of a failed sample showing the location of fractured fibres with bleeding-light.

Since a pair of AE transducers were surface-mounted on the specimen, linear-location of AE events was possible. The wave propagation speeds for the small-diameter optical fibre bundle and the composites were 4000 (±200) and 3500 (±200) metres per second respectively. These values agree with published data [5].

The data from the AE linear-location study is shown in Figure 10a, where the linear-location of the AE event is given in relation to the length of the tensile test specimen. Since the light emanating from the fracture of each of the small-diameter optical fibres is detectable visually, the fracture sequence of the fibres within the test specimen can be recorded. Figure 10b illustrates light bleeding from a failed test specimen.

CONCLUSIONS

As-received E-glass and custom-made small-diameter optical fibre bundles and their composites were evaluated. A technique was developed to fabricate void-free composites. Custom-made end-tabs were used to enable the samples to be gripped and tensile tested to failure without causing damage to the fibre light-guides in the grips. A pair of acoustic emission transducers was used to trigger the high-speed camera which in turn recorded the fracture of individual fibres in the bundle and composite. The feasibility of tracking the failure of each fibre during tensile loading was demonstrated. The image analysis routines developed could identify fibres just prior to failure, where an attenuation of the transmitted light intensity was observed. AE linear-location was seen to correlate with the visually observed location of fibre fracture as inferred by bleeding-light. It is now possible to correlate the effects of surface treatment and processing conditions to the fracture of glass fibre composites in real-time.

ACKNOWLEDGEMENTS

The authors would like to acknowledge the financial support from Engineering and Physical Sciences Research Council (EPSRC), the Ministry of Defense and the participating industrial sponsors.

References

1. Hayes, S., Liu, T., Brooks, D., Monteith, S., Ralph, B., Vickers, S. and Fernando, G. F. (1997), "In situ self-sensing fibre reinforced composites", Smart Materials and Structures, vol. 6, no. 4, pp. 432-440.

2. Fernando, G. F., Degamber, B., Wang, L., Doyle, C., Kister, G. and Ralph, B. (2004), "Self-sensing fibre reinforced composites", Advanced Composites Letters, vol. 13, no. 2, pp. 123-129.

3. Kister, G., Wang, L., Ralph, B. and Fernando, G. F. (2003), "Self-sensing E-glass fibre ", Optical Materials, vol. 21, no. 4, pp. 713-727.

4. Fernando, G. F., Crosby, P. A. and Liu, T. (1999), "The Application Of Optical Fibre Sensors In Advanced Fibre Reinforced Composites: Chapter 2 - Introduction And Issues", Optical Fibre Sensor Technology, Volume III, Edited by K. T. V. Grattan and B. T. Meggitt. Publisher: Kluwer Academic Publishers. ISBN 0412825708.

5. Mili R., Moevus, M., and Godin, N., (2008), "Statistical fracture of E-glass fibers using a bundle tensile test and acoustic emission monitoring", Composites Science and Technology, vol. 68, no. 7-8, pp. 1800-1808.